Gliosarcoma of the right cerebellar hemisphere and parahippocampal region: A case report and literature review

FA WU[1], YULIN YANG[2], ZAIQING WANG[3], RUI JIANG[1], TINGTING WU[1], TING YU[4] and PENG WANG[1]

[1]Department of Radiology, The General Hospital of Western Theater Command, Chengdu, Sichuan 610083, P.R. China;
[2]Department of Ultrasound, Longquanyi District First People's Hospital, Chengdu, Sichuan 610000, P.R. China;
[3]Department of Radiology, Chengdu Bayi Orthopedic Hospital, Chengdu, Sichuan 610100, P.R. China;
[4]Department of Pathology, The General Hospital of Western Theater Command, Chengdu, Sichuan 610083, P.R. China

Received September 25, 2025; Accepted January 23, 2026

DOI: 10.3892/ol.2026.15500

Abstract. Intracranial gliosarcoma (GSM) is a rare and aggressive variant of glioblastoma, characterized by a dismal prognosis and high rates of early recurrence and metastasis. Preoperative differentiation from other neoplasms based on imaging features remains a significant clinical challenge. The current study reports the case of a 55-year-old female who presented with a headache as the primary clinical symptom. The patient underwent brain MRI due to progressively worsening symptoms of diplopia, intermittent dull headaches localized to the right occipital region and an unsteady gait. Preoperative magnetic resonance imaging revealed a large, lobulated mass in the right cerebellar hemisphere extending into the parahippocampal region. The diagnosis of WHO Grade IV GSM was confirmed by postoperative histopathological and immunohistochemical analysis, which revealed a biphasic pattern with glial fibrillary acidic protein-positive glial and smooth muscle actin/vimentin-positive sarcomatous components, alongside a high Ki-67 proliferation index of 30%. The patient underwent a subtotal resection followed by adjuvant radiotherapy with concurrent temozolomide chemotherapy. Despite this multimodal treatment, follow-up imaging demonstrated tumor recurrence at 2 months, with significant further progression and brain herniation observed at the 12-month follow-up. The present case underscores the diagnostic challenges and aggressive clinical course of GSM, particularly when located in the cerebellum. The rapid recurrence despite combined-modality therapy highlights the need for improved diagnostic strategies and more effective treatment protocols for this formidable disease.

Correspondence to: Dr Peng Wang, Department of Radiology, The General Hospital of Western Theater Command, 270 Tianhui Road, Rongdu Avenue, Jinniu, Chengdu, Sichuan 610083, P.R. China
E-mail: kl415@qq.com

Key words: gliosarcoma, glioblastoma, magnetic resonance imaging, pathology, case report

Introduction

According to the 2021 World Health Organization (WHO) Classification of Tumors of the Central Nervous System, gliosarcoma (GSM) is a distinct histopathological variant of isocitrate dehydrogenase (IDH)-wild-type glioblastoma (GBM), categorized as a WHO Grade IV neoplasm, the highest malignancy grade for central nervous system tumors (1,2). Clinically, GSM is exceptionally rare, accounting for only 1.5-8% of all GBM cases, with a median onset age of ~52 years and a slight male predominance (male-to-female ratio, 1.2:1-1.5:1) (3-5). The prognosis is poor, with untreated patients having a median overall survival (OS) time of only 4 months. Even with standard multimodal therapy (following the Stupp protocol), the median OS time only extends to 6.6-18.5 months (most commonly 12-15 months) (6-8). Prognostic factors include tumor location (supratentorial lesions fare better than infratentorial ones), extent of surgical resection (gross-total resection improves survival) and molecular markers such as O^6-methylguanine-DNA methyltransferase promoter methylation (4,6,9).

The preoperative diagnosis of GSM is challenging due to non-specific clinical and imaging features. Clinically, supratentorial GSM typically causes seizures, focal neurological deficits or elevated intracranial pressure (headaches and nausea), while infratentorial cases may present with ataxia, diplopia or brainstem compression symptoms (10). Imaging often shows a heterogeneously enhancing mass with peritumoral edema, overlapping with malignant meningioma (distinguished by epithelial membrane antigen (EMA) positivity and glial fibrillary acidic protein (GFAP) negativity), anaplastic astrocytoma (no biphasic histology and lower Ki-67 index), or metastatic tumors (history of extracranial primary tumors and lineage-specific markers) (11-13). A definitive diagnosis relies on histopathology (biphasic glial-sarcomatous components) and immunohistochemistry (GFAP-positive glial cells, smooth muscle actin (SMA)/vimentin-positive sarcomatous cells) (12,13). Treatment primarily involves maximal safe surgical resection (often subtotal for deep/infratentorial lesions to preserve neural function), followed by adjuvant intensity-modulated radiotherapy (IMRT; total, 60 Gy in 30 fractions) and concurrent temozolomide chemotherapy

(75 mg/m^2 during radiotherapy, then 150-200 mg/m^2 for 5 days every 28 days for 6 cycles) (8,14),16,17). Despite this, >70% of patients experience recurrence within 12 months, with no standardized salvage therapy (6,15).

GSM most commonly arises in supratentorial regions (temporal, frontal and parietal lobes), with infratentorial (cerebellar and brainstem) cases accounting for <5% (3,9). This rarity, combined with the anatomical constraints of the posterior fossa, makes cerebellar GSM particularly challenging to diagnose and treat. The present study reports an unusual case of GSM originating in the right cerebellar hemisphere with extension to the parahippocampal region, detailing the patient's clinical presentation, comprehensive imaging findings, pathological characteristics, treatment course and outcomes. A review of the relevant literature is also included to enhance understanding of this rare tumor's behavior and management complexities.

Case report

Patient presentation. A 55-year-old woman presented to the General Hospital of Western Theater Command (Chengdu, China) in April 2022 with a 2-month history of diplopia. At 1 month prior to admission, the patient developed intermittent, dull headaches localized to the right occipital region. The symptoms progressively worsened, culminating in an unsteady gait with a tendency to tilt to one side. A physical examination revealed instability upon standing when the left eye was covered (positive Romberg sign), while stability was maintained with the right eye covered. The right finger-nose test was positive, indicating cerebellar dysfunction. No facial numbness, dysphagia or limb motor deficits were observed. Routine laboratory investigations were within normal limits. All imaging, neurosurgical procedures and pathological examinations were performed at the General Hospital of Western Theater Command. The patient was first admitted to the Department of Neurosurgery in April 2022. At 10 days post-admission, the patient underwent resection of the right cerebellar space-occupying lesion, craniotomy decompression and repair of cerebrospinal fluid leakage via the infratentorial supracerebellar approach. The operation lasted 6 h and 2 min, with a smooth procedure and satisfactory anesthesia effect. Intraoperative blood loss was 200 ml, and no blood transfusion was required. The patient regained spontaneous breathing uneventfully postoperatively. In August 2022, the patient subsequently received cranial radiotherapy combined with concurrent chemotherapy. The chemotherapeutic regimen consisted of oral temozolomide administered once daily, as later described. In March 2023, the patient returned to the Oncology Outpatient Department at the General Hospital of Western Theater Command for a follow-up magnetic resonance imaging (MRI) examination.

Imaging findings and follow-up. Preoperative brain MRI demonstrated a large (4.0x2.8x2.7 cm), lobulated, mixed-signal-intensity mass occupying the right cerebellar hemisphere and parahippocampal region. The lesion exhibited partial diffusion restriction on diffusion-weighted imaging/apparent diffusion coefficient sequences. Susceptibility-weighted imaging revealed intralesional punctate hypointensities suggestive of microhemorrhages or calcifications. Post-contrast T1-weighted imaging revealed marked heterogeneous enhancement. Significant perilesional edema, manifesting as T1 hypointensity and T2 hyperintensity, was noted in the adjacent cerebellar parenchyma, extending to involve the right brainstem and cerebellar vermis. Mass effect resulted in compression of the fourth ventricle. Magnetic resonance spectroscopy (MRS) within the lesion demonstrated a characteristically elevated choline (Cho) peak and a markedly reduced N-acetylaspartate (NAA) peak, consistent with high cellular turnover and neuronal loss. Patchy slightly prolonged T1 and isointense T1 signals were noted in the right cerebellar hemisphere and right parahippocampal region (Fig. 1A). On T2-weighted imaging, the same region exhibited slightly prolonged T2 signals interspersed with small patchy slightly shortened T2 signals (Fig. 1B), with a lobulated mixed-signal mass identified in this area. Susceptibility-weighted imaging revealed punctate hypointense foci within the lesion (Fig. 1C). Fluid-attenuated inversion recovery imaging showed hyperintense signals in the lesion (Fig. 1D). Marked heterogeneous enhancement of the lesion was seen on axial (Fig. 1E) and coronal (Fig. 1F) post-contrast images. The lesion involved the right brainstem and cerebellar vermis, with compression of the adjacent fourth ventricle and brainstem. MRS of the lesion area revealed a decreased NAA peak, a significant elevation of the Cho peak and a nearly unchanged creatine (Cr) peak (Fig. 1G).

At the 2-month postoperative follow-up, MRI confirmed tumor recurrence in the primary site. The recurrent lesion exhibited trans-tentorial extension, involving the right cerebellar tentorium and right brainstem, with persistent heterogeneous contrast enhancement (Fig. 2).

By the 12-month follow-up, the recurrent tumor had enlarged considerably, with further involvement of the right temporal lobe. The imaging revealed extensive perilesional edema, a significant mass effect with midline shift and evidence of brain herniation (Fig. 3).

Operative record. Under general anesthesia, the patient was positioned in a left lateral prone position with Mayfield head frame fixation. A right paramedian occipital straight incision was made. A craniotomy was performed, exposing the transverse sinus. Upon dural opening, significant cerebellar swelling and elevated intracranial pressure were noted. A subtentorial supracerebellar approach was utilized. After arachnoid dissection and mobilization of venous structures, a firm, poorly demarcated tumor was identified in the tentorial region. Due to persistent tension in the posterior fossa despite cerebrospinal fluid (CSF) release and dehydration, a complete dissection was deemed unsafe. An internal decompression was performed via piecemeal resection of the tumor and a portion of the cerebellar tissue. Meticulous dissection preserved the superior cerebellar artery and key venous structures. An attempt to access the supratentorial component via tentorial incision was limited by anatomical constraints, resulting in residual supratentorial tumor. Hemostasis was achieved, the dural defect was repaired with an artificial graft and the bone flap was secured. A surgical drain was placed before layered closure.

Immunohistochemistry. The postoperative tumor tissue was fixed in 10% neutral buffered formalin at 25˚C for 24 h, routinely

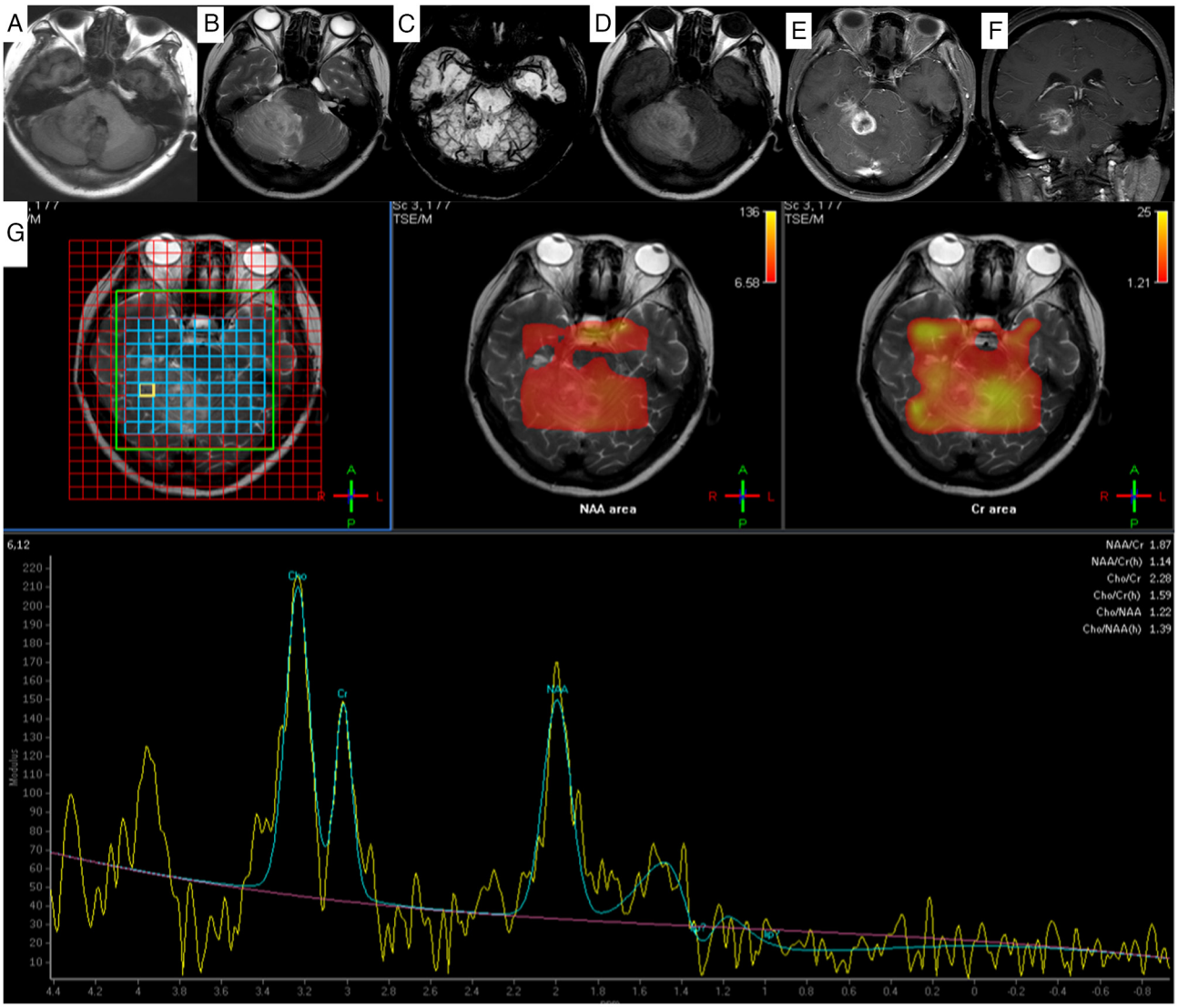

Figure 1. Magnetic resonance imaging findings of gliosarcoma in the right cerebellar hemisphere and right parahippocampal region. (A) In the right cerebellar hemisphere and right parahippocampal region, patchy slightly hyperintense and isointense signals on T1-weighted imaging were observed. (B) On T2-weighted imaging, slightly hyperintense signals were noted, mixed with small patchy slightly hypointense signals. (C) Susceptibility-weighted imaging demonstrates punctate hypointense foci within the lesion. (D) Fluid-attenuated inversion recovery imaging shows hyperintensity. The lesions exhibited obvious inhomogeneous enhancement on (E) axial and (F) coronal images. The lesion involves the right portion of the brainstem and cerebellar vermis, with compression of the adjacent fourth ventricle and brainstem. (G) The peak value of NAA in the lesion area was decreased, the peak value of Cho was significantly increased, and the peak value of Cr remained basically unchanged. MRI, magnetic resonance imaging; NAA, N-acetylaspartate; Cr, creatine; TSE/M, turbo spin echo/magnetization.

processed, paraffin-embedded and sectioned at a 4-μm thickness. Immunohistochemical staining was performed using the EnVision two-step method. Endogenous peroxidase activity was blocked with 3% hydrogen peroxide for 10 min at room temperature. Antigen retrieval was performed with heat induction using EDTA buffer (pH 9.0) at a constant temperature of 100˚C in a microwave, followed by graded alcohol rehydration. Sections were then blocked with normal goat serum (OriGene Technologies, Inc.) for 30 min at room temperature. Primary antibodies (all Fuzhou Maixin Biotechnology Development Co., Ltd.) were applied and incubated overnight at 4˚C in a humidified chamber. A detailed list of the antibodies, including the clones, dilutions and catalog numbers, is shown in Table I. Subsequently, the HRP-labeled secondary antibody from the EnVision kit (catalog no. KIT-5001; Fuzhou Maixin Biotechnology Development Co., Ltd.) was applied and incubated for 30 min at room temperature. Hematoxylin and eosin (H&E) staining was performed on the gliosarcoma tissues following a standardized protocol, with all procedures conducted at 25˚C unless otherwise specified. Freshly resected gliosarcoma tissues (≤3 mm in thickness) were fixed in 10% neutral buffered formalin (pH 7.4) at 25˚C for 24 h (a maximum fixation duration of 72 h was applied to avoid over-fixation), then processed for routine paraffin embedding. Serial 4-μm thick sections were cut using a rotary microtome, mounted on positively charged glass slides and baked at 60˚C for 30 min for adhesion. H&E staining was implemented using the Hematoxylin-Eosin Staining Solution (Shaanxi Medical Device Preparation No. 20180101, Xi'an Meijiajia, China) with the following steps: Xylene deparaffinization (10, 10 and 5 min); graded alcohol rehydration (100% ethanol, 2x5 min; 95% ethanol, 3 min; 85% ethanol, 3 min; and 75% ethanol,

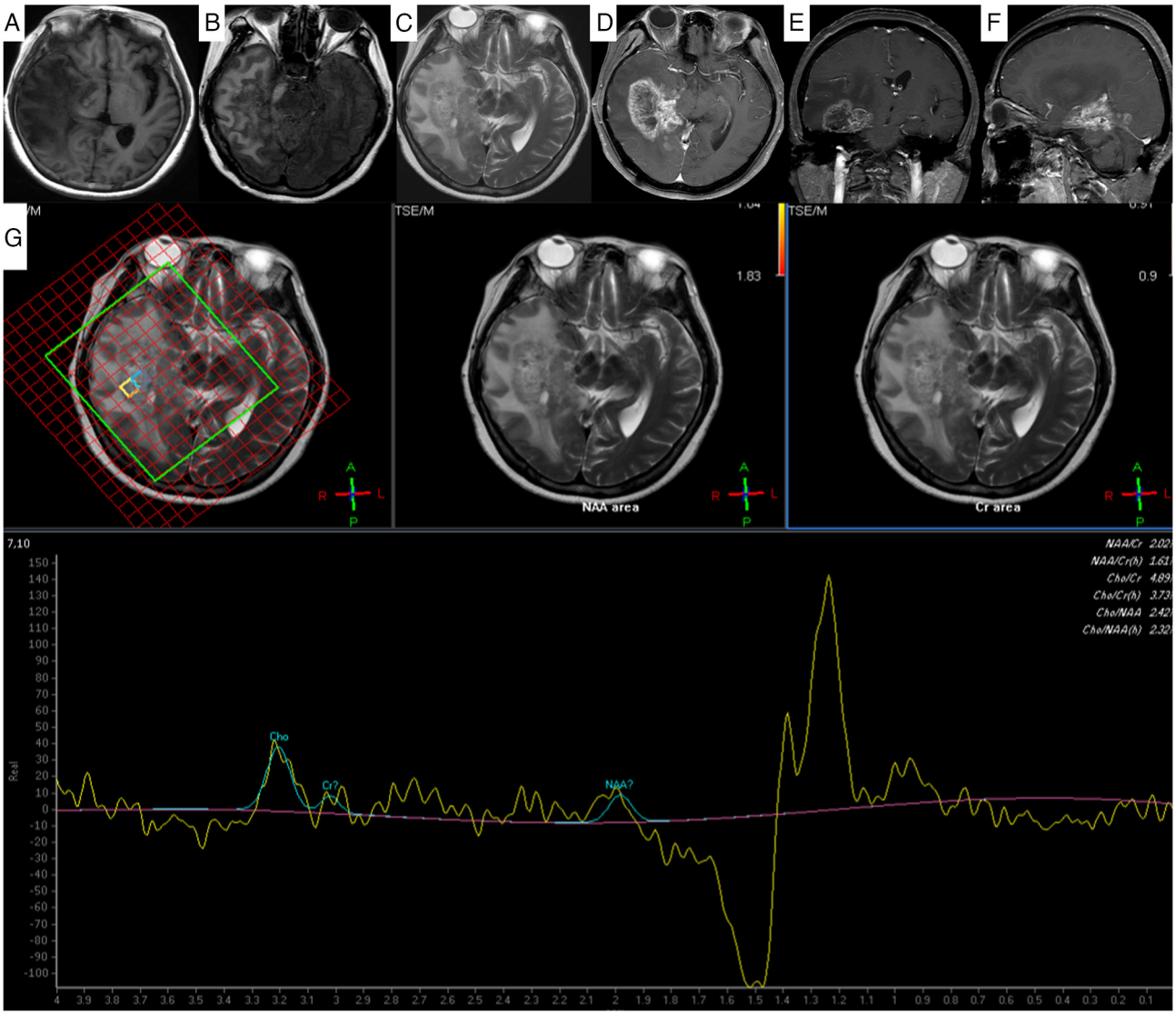

Figure 2. Recurrence of gliosarcoma on 2-month follow-up magnetic resonance imaging. A lobulated mixed-signal mass predominantly with (A) slightly long T1 and (B) slightly long T2 signals is present in the right cerebellar hemisphere and right parahippocampal region. (C) Fluid-attenuated inversion recovery imaging shows hyperintensity. After enhancement, the (D) axial, (E) sagittal and (F) coronal images of the lesion exhibited obvious inhomogeneous enhancement and annular enhancement. The lesion is growing across the tentorium, with thickening and significant enhancement of the adjacent right cerebellar tentorium; it involves the right portion of the brainstem, causing compression of the adjacent fourth ventricle and brainstem. (G) Magnetic resonance spectroscopy of the recurrent lesion reveals a decreased NAA peak and an increased Cho peak in the lesion area. The left panel shows the voxel placement (yellow grid). The middle and right panels display the spectrum without pseudo-color mapping, likely due to extremely low metabolite concentrations, incomplete water suppression (note the prominent water peak on the right), and/or post-processing thresholds. NAA, N-acetylaspartate; Cr, creatine; TSE/M, turbo spin echo/magnetization.

3 min); Harris hematoxylin staining (5-8 min); differentiation in 1% acid alcohol (3-5 sec); bluing in 0.5% lithium carbonate solution (10-20 sec); alcoholic Eosin Y staining (1-3 min); graded alcohol dehydration (95% ethanol, 3 min; 100% ethanol, 2x3 min); xylene clearing (2x5 min); and permanent mounting with neutral balsam. For immunohistochemical staining, the chromogenic reaction was visualized using a DAB substrate kit (cat. no. ab64238; Abcam), followed by hematoxylin counterstaining. All stained slides were examined under an Olympus BX53 bright-field light microscope (equipped with a DP74 digital camera; Olympus Corporation), and representative images were captured at magnifications of x100 (scale bar, 200 μm), x200 (scale bar, 100 μm) and x400 (scale bar, 50 μm; for identifying the biphasic glial and sarcomatous components) for documentation.

Pathological results. Histopathological examination confirmed the diagnosis of GSM (WHO Grade IV) (2). Macroscopically, the tumor was irregular with a firm, grey-brown cut surface. Microscopically, a biphasic pattern was evident, comprising both glial and sarcomatous components. The sarcomatous areas consisted of densely packed, fascicularly arranged spindle cells with abundant cytoplasm and prominent stromal vascular proliferation. The glial component was composed of fibrillary and gemistocytic astrocytoma cells, arranged in nests and diffuse sheets, with frequent mitotic figures (Fig. 4B and C).

Immunohistochemical staining was critical for establishing the definitive diagnosis. The staining profile revealed a distinct immunophenotype: The neoplastic cell exhibited focal positivity for calponin and GFAP (Fig. 4D), weak positivity for S-100 (Fig. 4E) and strong, diffuse positivity for smooth

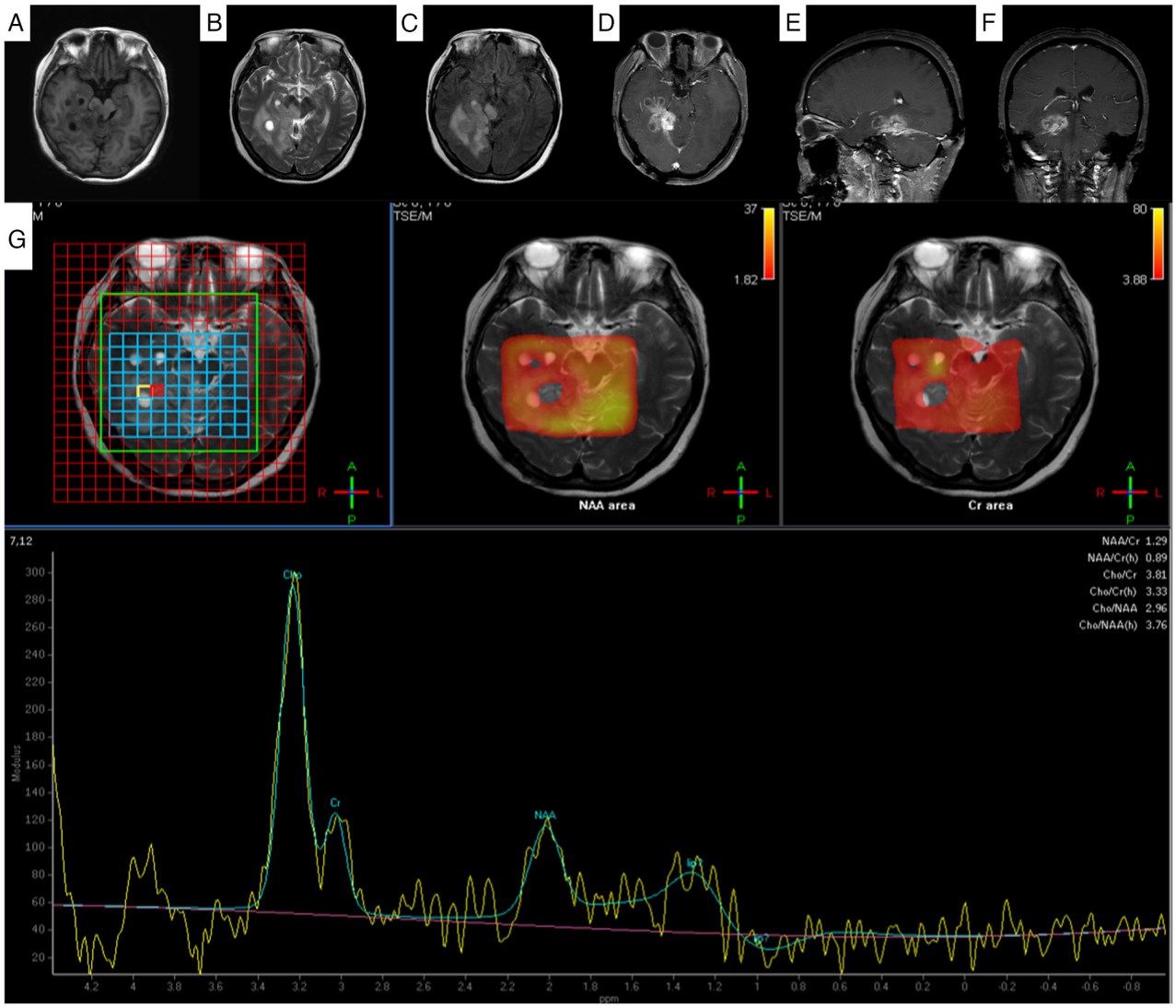

Figure 3. Enlargement of the recurrent gliosarcoma with brain herniation formation on 1-year follow-up magnetic resonance imaging. The dura mater in the right occipital region was thickened with obvious enhancement. The right cerebellar hemisphere, right parahippocampal region and right temporal lobe exhibited patchy mixed signal shadows. (A) On the T1WI sequence, slightly longer T1 signals were observed, and (B) on the T2WI sequence, slightly longer T2 signals were observed. (C) Fluid-attenuated inversion recovery imaging shows isointense and slightly hyperintense signals. After enhancement, the (D) axial, (E) sagittal and (F) coronal images of the lesion exhibited obvious inhomogeneous enhancement and annular enhancement. The lesion grows across the tentorium, with thickening and significant enhancement of the adjacent right cerebellar tentorium; it involves the right portion of the brainstem, causing compression of the adjacent fourth ventricle, right lateral ventricle and brainstem, with leftward shift of the midline structures. (G) Magnetic resonance spectroscopy reveals a decreased NAA peak and an increased Cho peak in the lesion area. NAA, N-acetylaspartate; Cr, creatine; TSE/M, turbo spin echo/magnetization.

muscle actin (SMA) and vimentin (Fig. 4F and G, respectively). A high proliferative index was indicated by a Ki-67 labeling index of 30% (Fig. 4H). Furthermore, the tumor cells were consistently negative for a panel of markers including caldesmon, CD34, cytokeratin (CK), EMA and progesterone receptor, as illustrated in Fig. 4I-M. This combined pattern of strong co-expression of SMA and vimentin with a high Ki-67 index, alongside the absence of specific lineage markers, was instrumental in narrowing the differential diagnosis.

Postoperative treatment. Before radiotherapy, a head CT scan was performed using a helical tomotherapy system (Accuray, Inc.). The scanning parameters were as follows: The patient was positioned in a supine position, utilizing helical scanning with a tube voltage of 120 kV, tube current ranging from 200 to 250 mAsec and a slice thickness of 1 mm. The scanning range extended 2 cm from the upper edge of the parietal scalp to the lower part of the skull base. This scan was conducted for radiotherapy localization. The patient subsequently received adjuvant IMRT concurrent with daily oral temozolomide at a dose of 100 mg for a total of 38 days. The planning target volume (PTV) for the postoperative bed (PTV1) received 6,500 cGy in 30 fractions, while the adjacent brainstem region (PTV2) received 5,200 cGy (max dose, 5,358.8 cGy) (Fig. 5). Supportive care included intravenous administration of 20% mannitol (a routine dehydrating agent for cerebral edema) at a dose of 250 ml per infusion, administered every 8 h (1-2 g/kg body weight) via rapid intravenous drip (completed within 30-60 min), for a total of 38 consecutive days.

Follow-up and outcome. The patient's most recent follow-up was in March 2023. At that time, a neurological examination

Table I. Antibodies for immunohistochemistry.

Antibody	Clone number	Recommended dilution	Catalog number	Supplier
Actin	MX083	1:100	MAB-0871	Fuzhou Maixin Biotech Co., Ltd.
CD34	QBEnd/10	Ready-to-use	Kit-0004	Fuzhou Maixin Biotech Co., Ltd.
Pan-CK	AE1/AE3	Ready-to-use	0349	Shanghai Long Island Antibody Diagnostica Inc.
Caldesmon	MX077	1:50	MAB-0865	Fuzhou Maixin Biotech Co., Ltd.
Calponin	MX023	1:100	MAB-0712	Fuzhou Maixin Biotech Co., Ltd.
Desmin	MX046	1:50	MAB-0766	Fuzhou Maixin Biotech Co., Ltd.
EMA	MX132E29	Ready-to-use	MAB-1101	Fuzhou Maixin Biotech Co., Ltd.
ER	MXR030	1:50	RMA-1065	Fuzhou Maixin Biotech Co., Ltd.
GFAP	MX-047	Ready-to-use/1:100	MAB-0769	Fuzhou Maixin Biotech Co., Ltd.
Ki-67	MX-006	Ready-to-use/1:50	MAB-0672	Fuzhou Maixin Biotech Co., Ltd.
PR	MXR008	1:50	RMA-0895	Fuzhou Maixin Biotech Co., Ltd.
S-100	rMM-S1	Ready-to-use/1:100	0466	Shanghai Long Island Antibody Diagnostica Inc.
SMA	1D6	Ready-to-use/1:100	MAB-0575	Fuzhou Maixin Biotech Co., Ltd.
SOX-10	MXR026	1:100	RMA-1058	Fuzhou Maixin Biotech Co., Ltd.
STAT-6	YE361	1:100	YE361	Abcam Shanghai Trading Co., Ltd.
Vim	MX034	Ready-to-use/1:200	MAB-0735	Fuzhou Maixin Biotech Co., Ltd.

CK, cytokeratin; EMA, epithelial membrane antigen; ER, estrogen receptor; GFAP, glial fibrillary acidic protein; PR, progesterone receptor; SMA, smooth muscle actin; SOX-10, SRY-box transcription factor 10; STAT6, signal transducer and activator of transcription 6; Vim, vimentin.

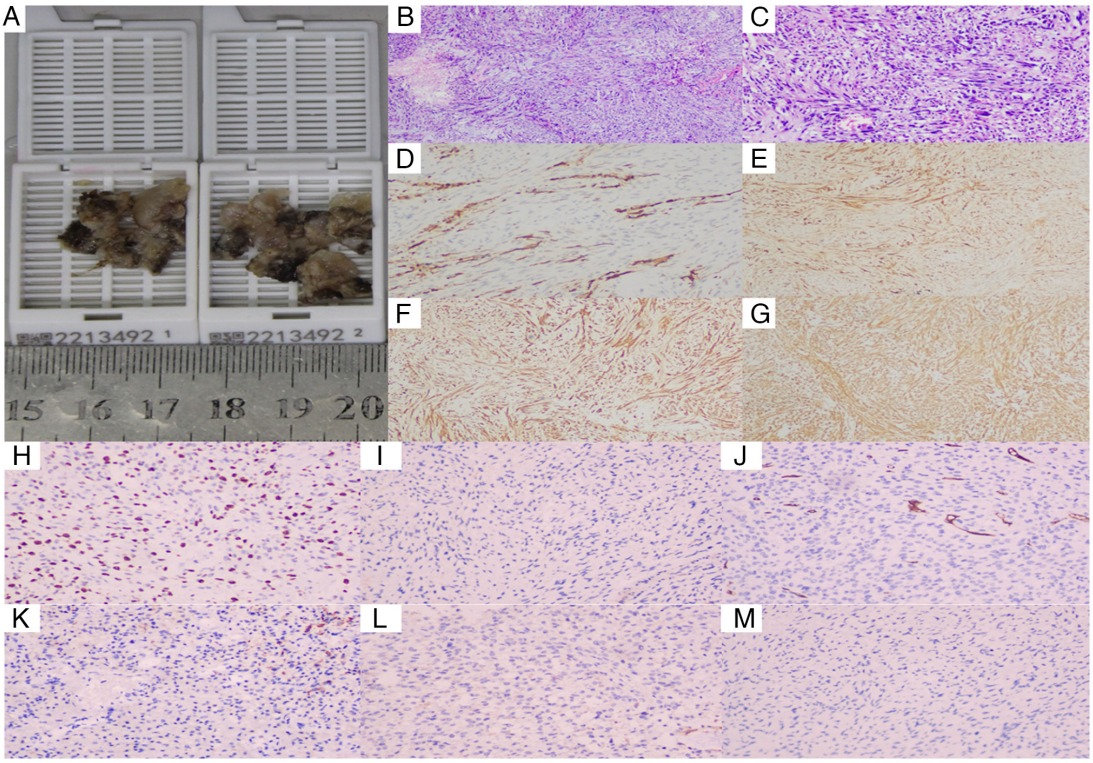

Figure 4. Pathological images of the resected gliosarcoma. (A) The tumor displays an irregular morphology with a grey-brown cut surface and firm consistency. (B and C) Hematoxylin and eosin-stained tissue samples at (B) x40 and (C) x100 magnification. The tumor is composed of dual components: Glial and sarcomatous. The sarcomatous component exhibits a spindle cell sarcoma pattern, characterized by densely packed long fascicles of spindle cells arranged in fascicular or small cluster-like configurations, abundant cytoplasm and prominent stromal vascular proliferation. (D) Glial fibrillary acidic protein positivity (x200 magnification). (E) Weak positivity for S-100 (x200 magnification). (F) Smooth muscle actin positivity (x200 magnification). (G) Vimentin positivity (x200 magnification). (H) Ki-67 positivity (30%) (x200 magnification). (I) Caldesmon negativity (x200 magnification). (J) CD34 negativity (x200 magnification). (K) Cytokeratin negativity (x200 magnification). (L) Epithelial membrane antigen negativity (x200 magnification). (M) Progesterone receptor negativity (x200 magnification).

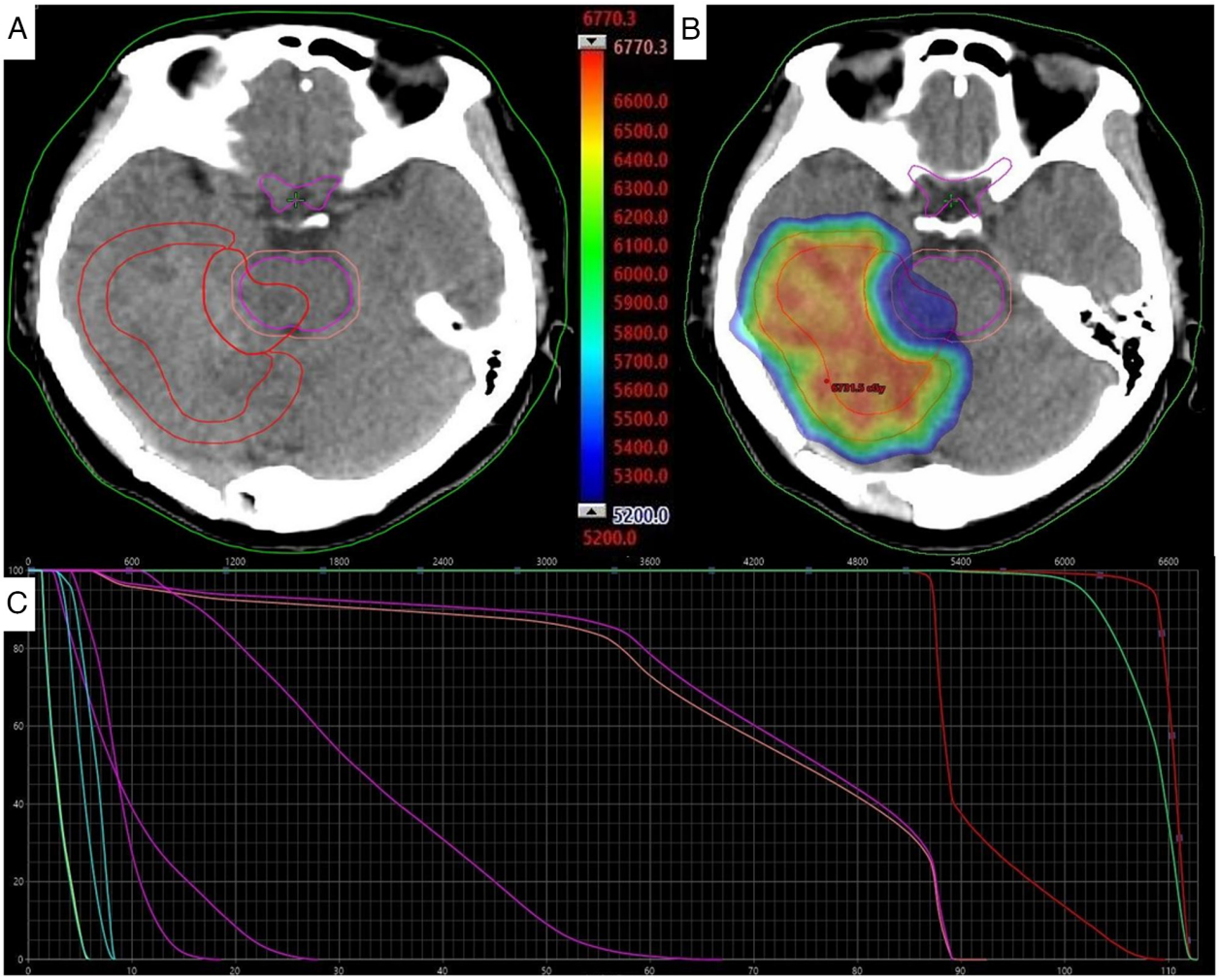

Figure 5. Intracranial lesion radiotherapy treatment plan. (A) Target delineation: The GTVs were defined as GTV-65 (intracranial lesions outside the brainstem) and GTV-53 (brainstem lesions). The planning target volumes were generated by expanding the respective GTVs by 0.8 cm, and the brainstem interface was not expanded. (B) The dose distribution was shown on the axial computed tomography slices with equal dose, and the total dose was 6,731.5 cGy. (C) Dose-volume histogram of target volume and organs at risk; dosage limits for dangerous organs follow the Radiation Therapy Oncology Group guidelines (18). GTV, gross tumor volume.

revealed mild limitations to the downward movement in the right eye, a positive right finger-nose test and a positive Romberg sign, indicating persistent cerebellar dysfunction. No significant abnormalities were noted on routine laboratory tests. However, follow-up MRI demonstrated significant enlargement and progression of the recurrent lesion in the right cerebellar hemisphere and parahippocampal region, with suspected brainstem invasion. This rapid progression, observed despite combined modality therapy, underscores the highly aggressive nature of cerebellar GSM.

Following this last evaluation, the patient's condition continued to deteriorate due to disease progression, and the patient succumbed to the disease in July 2023. This outcome further underscores the dismal prognosis associated with this aggressive tumor variant, particularly when located in the posterior fossa.

Discussion

GSM has a poor prognosis with high recurrence rates (15), as illustrated in the present case, where the disease progressed rapidly leading to a poor clinical status by the last follow-up in March 2023. Untreated patients have a median overall survival time of 4 months, while combined modality therapy extends this to 6.6-18.5 months (7). GSM is a highly aggressive tumor with a median age of onset of ~52 years and a slight male predominance (4). The clinical course is typically rapid, characterized by significant mass effect and peritumoral edema. Symptoms are directly related to the tumor's location and invasion of adjacent structures, often leading to elevated intracranial pressure (10). The current patient's presentation with diplopia and occipital headaches is consistent with this profile, exacerbated by the rare cerebellar location causing brainstem compression. Beyond symptomatology, this anatomical distinction fundamentally impacts therapeutic strategy. The compact anatomy of the posterior fossa and proximity to critical brainstem structures often preclude the aggressive surgical margins achievable in non-eloquent supratentorial regions. Consequently, the surgical goal in cerebellar GSM frequently shifts from a gross-total resection to maximal safe debulking and cytoreduction, inherently increasing the risk of local recurrence due to residual disease burden.

MRI is the cornerstone of preoperative evaluation for GSM. GSM typically presents as a heterogeneously enhancing mass with ill-defined margins, marked edema and frequent dural attachment, which can mimic a malignant meningioma (11). Signal characteristics often include T1 hypointensity, T2 hyperintensity and heterogeneous post-contrast enhancement, occasionally with a 'reticular' pattern (16). MRS consistently shows an elevated Cho/NAA ratio, reflecting high cellularity and malignancy (17). The present case exhibited these typical features, alongside the unusual finding of a large cerebellar location and trans-tentorial spread.

The aggressive course observed in the present patient, characterized by early recurrence and trans-tentorial spread, can be critically contextualized within the broader literature on GSM. While the biphasic histology and poor prognosis are consistent with the defining features of GSM (1,12,13), several aspects of the present case highlight its distinctiveness and amplify its clinical challenge.

GSM most frequently arises in supratentorial locations, particularly the temporal lobe, with cerebellar origins being exceptionally rare (3,4). This anatomical distinction is not merely incidental. Supratentorial GSM, while aggressive, often permits a more extensive surgical resection in non-eloquent areas. By contrast, in the present case, the origin in the cerebellar hemisphere, with immediate proximity to and compression of the brainstem, inherently limited the goal of surgery to a subtotal resection for decompression. This unavoidable surgical constraint likely contributed to the high residual tumor burden, a factor strongly associated with early recurrence in GBM and its variants (6,9). The presenting symptoms of ataxia and brainstem compression are direct manifestations of this location, differing from the more common seizures or focal neurological deficits seen in temporal lobe GSM (10).

The Ki-67 proliferation index of 30% in the present case is at the higher end of the spectrum reported for GSM (typically ranging from 15 to 30%) (4,13). This elevated proliferative activity provides a histopathological link to the explosively aggressive behavior observed radiologically, including the rapid trans-tentorial extension noted at the 2-month follow-up. This pattern of spread is less commonly detailed in reports of supratentorial GSM but may be facilitated in cerebellar cases by anatomical routes along the tentorium. Furthermore, the marked perilesional edema and heterogeneous 'reticular' enhancement pattern on MRI, as seen in the present patient, are features described in GSM series (11,17). However, when these features occur in the posterior fossa, the resultant mass effect on the brainstem and fourth ventricle carries more immediate life-threatening implications, such as herniation, which ultimately occurred in the present patient at 12 months postoperatively.

The median overall survival time for GSM treated with multimodal therapy is 6.6-18.5 months (6,7). In the present patient, the rapid progression leading to brain herniation at 12 months aligns with the poorer end of this spectrum. This outcome underscores that cerebellar GSM may confer an even worse prognosis than its supratentorial counterparts, a hypothesis supported by the compounded challenges of limited resectability and critical adjacent neuroanatomy. This aligns with findings of the study by Feng *et al* (9), which identified tumor location as a significant prognostic factor in a nomogram analysis.

Pathologically, GSM is defined by its biphasic glial ($GFAP^+$) and sarcomatous ($vimentin^+/SMA^+$) morphology (1,12,13).

There is no standardized treatment protocol for GSM. Maximal safe surgical resection remains the primary treatment, followed by adjuvant chemoradiotherapy, mirroring the Stupp protocol for GBM (8,9). High-dose radiotherapy and combined modality therapy have been identified as favorable prognostic factors (14). Despite aggressive therapy, the prognosis remains poor, with a median overall survival time of 6.6-18.5 months and high recurrence rates (6). The early recurrence in the present patient, despite combined-modality therapy, can be attributed to the tumor's critical location limiting the extent of resection and its inherent high malignancy, potentially with early CSF dissemination.

In conclusion, the present study highlights a rare case of cerebellar GSM with classic biphasic pathology and a highly aggressive clinical course. Preoperative imaging, while suggestive of a high-grade glioma, is non-specific, and a definitive diagnosis relies on thorough histopathological and immunohistochemical evaluation. The rapid recurrence and progression observed in the present patient, despite multimodal therapy, underscore the therapeutic challenges posed by GSM and emphasize the urgent need for novel diagnostic and treatment strategies to improve patient outcomes.

Acknowledgements

The authors would like to thank Dr Yihao Peng (Department of Radiology, The General Hospital of Western Theater Command, Chengdu, China) and Dr Jie Wu (Department of Radiology, The General Hospital of Western Theater Command) for the collection, sorting and verification of radiological and histopathological data.

Funding

This research was supported by the Foundation of General Hospital of Western Theater Command (grant no. 2024-YGLC-B07).

Availability of data and materials

The data generated in the present study are included in the figures and/or tables of this article.

Authors' contributions

FW, YY, ZW, RJ designed the study and conceptual framework. FW performed clinical data collection and case follow-up, PW advised on patient treatment and analyzed patient data, and YY and ZW assisted with clinical data collection. FW, PW and TY obtained clinical specimens, performed imaging and conducted the pathological analysis. FW sorted and verified the case data, and PW, YY, RJ and TW analyzed and organized the patient data. FW, PW and RJ drafted the case description and manuscript composition. PW, YY and TY revised the manuscript and provided academic polishing. FW, YY, RJ and PW prepared imaging, pathological figures and tables. FW,

PW and TY provided study design oversight and clinical guidance. Project administration was performed by PW. Funding acquisition was the responsibility of FW. All authors have read and approved the final manuscript. FW and TY confirm the authenticity of all the raw data.

Ethics approval and consent to participate

Not applicable.

Patient consent for publication

Written informed consent for the publication of this case report and accompanying images was obtained from the patient prior to her death.

Competing interests

The authors declare that they have no competing interests.

References

1. Louis DN, Perry A, Reifenberger G, von Deimling A, Figarella-Branger D, Cavenee WK, Ohgaki H, Wiestler OD, Kleihues P and Ellison DW: The 2016 world health organization classification of tumors of the central nervous system: A summary. Acta Neuropathol (Berl) 131: 803-820, 2016.
2. Louis DN, Perry A, Wesseling P, Brat DJ, Cree IA, Figarella-Branger D, Hawkins C, Ng HK, Pfister SM, Reifenberger G, *et al*: The 2021 WHO classification of tumors of the central nervous system: A summary. Neuro Oncol 23: 1231-1251, 2021.
3. Gerges C, Elder T, Penuela M, Rossetti N, Maynard M, Jeong S, Wright CH, Wright J, Zhou X, Burant C, *et al*: Comparative epidemiology of gliosarcoma and glioblastoma and the impact of Race on overall survival: A systematic literature review. Clin Neurol Neurosurg 195: 106054, 2020.
4. Chen L, Rizk E, Sherief M, Chang M, Lucas CH, Bettegowda C, Croog V, Mukherjee D, Rincon-Torroella J, Kamson DO, *et al*: Molecular characterization of gliosarcoma reveals prognostic biomarkers and clinical parallels with glioblastoma. J Neurooncol 171: 403-411, 2024.
5. Karasev S, Talybov R, Chertoyev S, Trofimova T, Mochalov V, Kleshchevnikova T, Loginova N and Karaseva I: Diagnostic challenges of gliosarcoma: Case report of a rare glioblastoma histopathological variant. Front Radiol 5: 1687401, 2025.
6. Wang X, Jiang J, Liu M and You C: Treatments of gliosarcoma of the brain: A systematic review and meta-analysis. Acta Neurol Belg 121: 1789-1797, 2020.
7. La Torre D, Della Torre A, Lo Turco E, Longo P, Pugliese D, Lacroce P, Raudino G, Romano A, Lavano A and Tomasello F: Primary intracranial gliosarcoma: Is it really a variant of glioblastoma? an update of the clinical, radiological, and biomolecular characteristics. J Clin Med 13: 83, 2024.
8. Hashmi FA, Salim A, Shamim MS and Bari ME: Biological characteristics and outcomes of gliosarcoma. J Pak Med Assoc 68: 1273-1275, 2018.
9. Feng SS, Li HB, Fan F, Li J, Cao H, Xia ZW, Yang K, Zhu XS, Cheng TT and Cheng Q: Clinical characteristics and disease-specific prognostic nomogram for primary gliosarcoma: A SEER population-based analysis. Sci Rep 9: 10744, 2019.
10. Saki A, Faghihi U and Balde I: Differentiating gliosarcoma from glioblastoma: A novel approach using PEACE and XGBoost to deal with datasets with ultra-high dimensional confounders. Life (Basel) 14: 882, 2024.
11. Wang Y and Zhang Z: A case report: Gliosarcoma associated with a germline heterozygous mutation in MSH2. Front Neurol 15: 1388263, 2024.
12. Jiang NN, Larrazabal R, Alsunbul W and Lu JQ: Multiple pathological components in gliosarcoma. J Biomed Res 35: 408-410, 2020.
13. Castelli J, Feuvret L, Haoming QC, Biau J, Jouglar E, Berger A, Truc G, Gutierrez FL, Morandi X, Le Reste PJ, *et al*: Prognostic and therapeutic factors of gliosarcoma from a multi-institutional series. J Neurooncol 129: 85-92, 2016.
14. Adeberg S, Bernhardt D, Harrabi SB, Diehl C, Koelsche C, Rieken S, Unterberg A, von Deimling A and Debus J: Radiotherapy plus concomitant temozolomide in primary gliosarcoma. J Neurooncol 128: 341-348, 2016.
15. Xu L, Yang Z, Chen H, Sun C, Tu C, Gu Z and Luo M: Conditional survival and changing risk profile in patients with gliosarcoma. Front Med (Lausanne) 11: 1443157, 2024.
16. Martinez A, Binks S, Pumarola M, Hardas A, Easton A, Campo L, Browne M, Martins S, Garosi LS, Di Dona F and Tauro A: Gliosarcoma associated with bilateral hippocampal sclerosis in a cat presenting complex partial seizures with orofacial involvement: A case report. Clin Case Rep 12: e9123, 2024.
17. Fukada A, de Souza Queiroz L and Reis F: Gliosarcomas: Magnetic resonance imaging findings. Arq Neuropsiquiatr 78: 112-120, 2020.
18. Gondi V, Bauman G, Bradfield L, Burri SH, Cabrera AR, Cunningham DA, Eaton BR, Hattangadi-Gluth JA, Kim MM, Kotecha R, *et al*: Radiation therapy for brain metastases: An ASTRO clinical practice guideline. Pract Radiat Oncol 12: 265-282, 2022.